2-(2,4-Dinitrobenzyl)pyridine (DNBP): A Potential Light-Activated Proton Shuttle

by **Catrin Goeschen**[a]), **Rainer Herges***[a]), **Josef Richter**[b]), **Bogdan Tokarczyk**[b])[1]), and **Jakob Wirz***[b])

[a]) Institut für Organische Chemie, Christian-Albrechts-Universität, Otto-Hahn-Platz 4, D-24098 Kiel (phone: +49 431 880 2440; fax: +49 431 880 1558; e-mail: Rainer.Herges@gmail.com)

[b]) Departement Chemie, Klingelbergstrasse 80, CH-4056 Basel (phone: +41 76 413 4748; e-mail: J.Wirz@unibas.ch)

The well-known photochromic tautomerism of 2-(2,4-dinitrobenzyl)pyridine (**1**; CH; *Scheme* 1) was re-investigated by flash photolysis in aqueous solution in view of its potential application as a light-activated proton pump. Irradiation of **1** yields the enamine tautomer NH ($\lambda_{max} = 520$ nm) that rapidly equilibrates with its conjugate base CNO^- ($\lambda_{max} = 420$ nm). The pH–rate profile for the first-order decay of NH and CNO^- provides a direct determination of the acidity constant of NH, $pK_{a,c}^{NH} = 5.94 \pm 0.12$ ($I =$ 0.1M) and serves to clarify the mechanisms of proton transfer prevailing in aqueous solutions. The acidity constant of protonated **1** ($CHNH^+$), $pK_{a,c}^{CHNH} = 4.18 \pm 0.02$, was determined by spectrophotometric titration.

1. Introduction. – In 1925, *Tschitschibabin et al.* [1] reported that exposure of the pale yellow crystals of 2-(2,4-dinitrobenzyl)pyridine (**1**; labeled CH in *Scheme 1*) to sunlight developed a blue color that faded away within a day in the dark. They tentatively identified the blue product as the enamine tautomer NH. Irradiation of 2-nitrobenzyl compounds such as **1** generally yields the corresponding *aci*-nitro compounds by H-atom transfer from the *ortho*-alkyl group to the NO_2 group [2]. Thus, the tautomer OH is the expected primary photoproduct of **1** (CH) [3]. But numerous studies have confirmed the original assignment identifying the long-lived blue photoisomer as the enamine tautomer NH. Its absorption spectrum ($\lambda_{max} \approx 520$ nm in aqueous solution, 530–580 nm in other media) is similar to that of the corresponding *N*-methylated enamine NMe [1][4][5]. IR- and NMR-spectral data [6], and time-resolved resonance *Raman* [7] and polarized optical absorption spectra of oriented molecules [8] all confirm that the blue isomer is NH, and X-ray analysis recently established this structure [9]. Studies of **1** by flash photolysis [10–14] with sufficient time resolution [12–14] have identified OH as the primary photoproduct ($\lambda_{max} \approx$ 410 nm) that is subsequently converted to NH in a thermal reaction. Delayed formation of the enamine NH in MeCN was proposed to occur by proton transfer through the solvent [7b], but calculations and experiments indicate that intramolecular proton transfer OH → NH is also feasible (see *Sect. 2.1*). In fact, both pathways may be operating; *Kleinschmidt* and *Graness* [5] report a quantum yield of 0.019 for formation of NH *via* OH, and of 0.024 for a 'direct' formation of NH from **1**. According to calculations (see *Sect. 2.1*), the thermochemical, direct (suprafacial, *Woodward*–

[1]) Present address: Institute of Forensic Research, Westerplatte 9, PL-31-033 Krakow.

Hoffmann-forbidden) proton transfer NH → CH has a high activation barrier. A two-step reaction NH → [OH] → CH involving the short-lived and highly acidic OH intermediate (*aci*-nitro form) is clearly more favorable. Theoretical calculations on the photochemical CH → NH conversion [15] revealed that there is almost no barrier to this proton transfer on the S_1 excited-state hypersurface. In the present work focusing on transient intermediates on the millisecond time scale, the primary product OH was not observed.

Scheme 1. *The Three Tautomers of* **1**. The symbols CH, NH, and OH designate the position of the mobile proton.

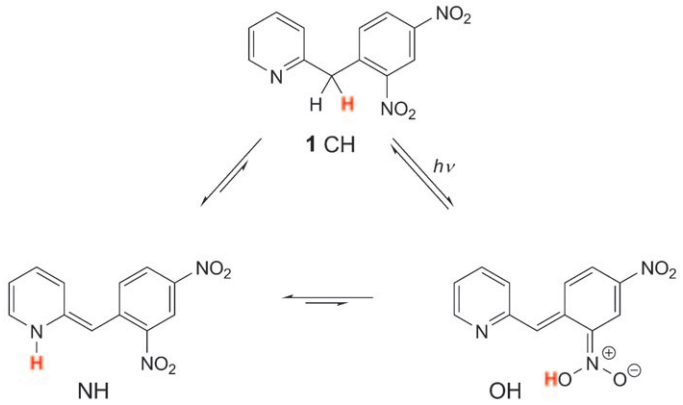

DNBP was extensively investigated for its potential use as a photochromic material [16]. It has been shown to switch the second-harmonic generation efficiency upon photoinduced isomerization and thus would be suitable as a nonlinear-optics material for holography and data-storage applications [17]. We here are planning to exploit the fact that DNBP reversibly switches its acid–base properties to design a proton shuttle. The two best-known systems that are capable to use light energy to pump protons uphill against a concentration gradient through a membrane are the photosynthetic reaction center and the bacteriorhodopsin in halophilic bacteria. Artificial photosynthesis has been achieved in a number of model systems [18]. The proton pump in these systems is driven by photoinduced electron transfer (for a recent review, see [19]). To the best of our knowledge, a proton pump based on a photoswitchable acid shuttle has only been presented once in the literature [20]. *Fig. 1* depicts the basic principle of our model system.

DNBP has a low polarity and dissolves in a lipophilic membrane that separates two aqueous phases. At pH < 4, its stable form is *N*-protonated $CHNH^+$. Upon irradiation of one of the phase boundaries (*Fig. 1*, right), it isomerizes to the *O*-protonated form, which is much more acidic and would release a proton to the aqueous phase. The remaining NH isomer is metastable, would diffuse through the membrane, and isomerize to the more basic CH form that would take up a proton at the other phase boundary. To determine optimal parameters for a light driven, uphill transport, the pK_a values and lifetimes of all species involved have to be known and, if necessary, optimized by structure variation.

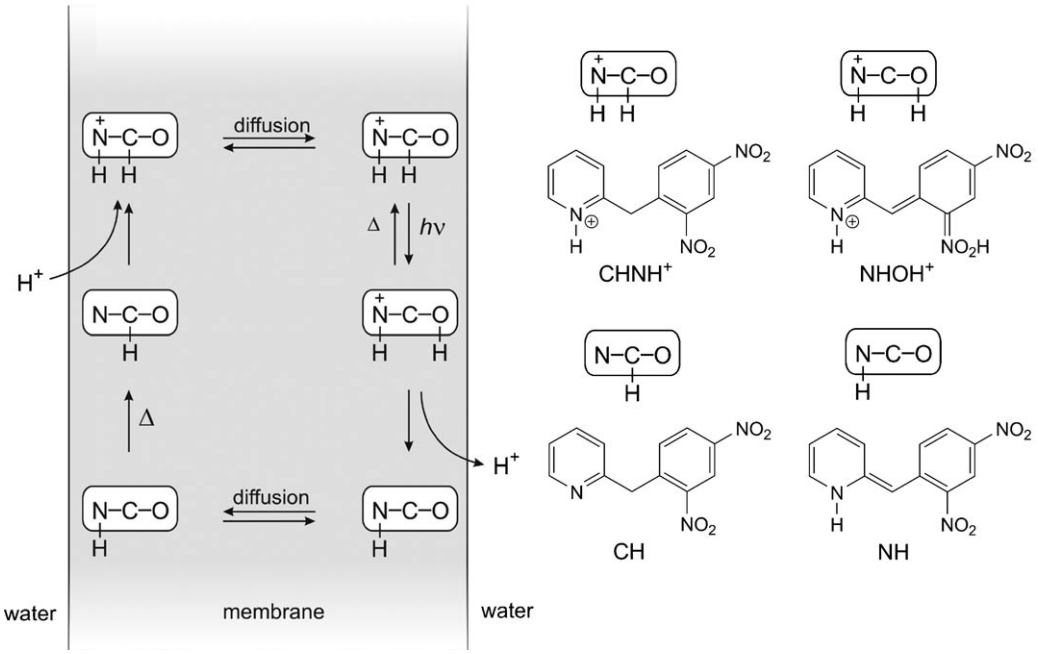

Fig. 1. *Hypothetical use of DNBP as a light-driven proton shuttle*

Wettermark measured rate constants for the thermal back reaction NH → CH in aqueous AcOH buffer solutions using flash photolysis [11]. *More O'Ferrall* and *Quirke* subsequently determined the rates for the forward reaction CH → NH under the same conditions by trapping the enamine intermediate NH with iodine [21]. By combining the rate constants for the forward and backward reaction, they determined the equilibrium constant for the tautomerization CH → NH, $pK_T^{NH} = 8.1$. The present study corroborates and extends the pioneering work of *Wettermark*, and of *More O'Ferrall* and *Quirke*. The thermodynamic and kinetic properties of the enamine NH in aqueous solution are characterized in detail.

2. Results. – 2.1. *Theoretical Calculations.* The mechanism of the light-induced proton transfer and the thermal back reaction of **1** have been investigated at several levels of theory. In 1996, semiempirical PM3 calculations were performed [15] to optimize the geometries and to determine the relative energies of the CH, OH, and NH forms, and the transition states between them. The excited-state energy hypersurface was investigated using multireference CI calculations (PM3-MRD-CI). *Ab initio* [22] and DFT calculations [8] confirmed the semiempirical data, except for the energy of the OH form and of the OH → NH transition state. The deviation of PM3 is probably due to the lack of adequate parameters for the protonated nitro group. The DFT calculations by *Naumov et al.* [8] predict the relative energies of the lowest-energy CH, OH, and NH isomers as 0.0, 82.7, and 50.7 kJ mol^{-1}, respectively. There are two different conformers of the OH form. One of them is connected *via* a transition state to

the NH form, and the other to the CH form. However, the energy hypersurface is extremely flat between the two conformers, which mainly differ by rotation around the *aci*-nitro group. The barrier for the CH → OH conversion was determined as 147 kJ mol^{-1}. On the other hand, there is either no or an extremely low barrier from the OH form to the NH isomer (rotation of the nitro group and proton transfer from the nitro group to the pyridine N-atom is probably simultaneous). The direct proton transfer from CH to NH has the very large activation energy of 229 kJ mol^{-1}, indicating that the indirect path NH → OH → CH is preferred over the NH → CH transfer. A molecular-dynamics simulation is in agreement with this picture [23].

We were able to reproduce the DFT data of *Naumov et al.* within a maximum error of 12 kJ mol^{-1} using the B3LYP/6-31G* level of density-functional theory and, in addition, also calculated the protonated species $CHNH^+$, $NHOH^+$, and the transition state between these two isomers (*Table 1*). The energy difference between the most stable protonated form $CHNH^+$ and the *O*-protonated form $NHOH^+$ is similar to the relative energies of the unprotonated species CH and OH. The same is true for the transition state.

Table 1. *Calculated Absolute* (a.u.) *and Relative Energies* (kJ mol^{-1} with respect to the most stable isomer) *of the Neutral and Protonated Species Including the Transition States at the B3LYP/6-31G* Level of Theory*

Structure[a])	$-E_{abs}$	E_{rel}	$-(E_{abs}+ZPE)$	E_{rel}
CH	927.6502847	0	927.4463	0
CH2	927.6484487	4.8	927.444669	4.3
NH	927.6253712	65.4	927.421289	65.6
NH2	927.6266777	14.81	927.422594	62.0
OH2	927.5982611	136.6	927.396252	131.4
TS CH → NH	927.5588405	240.1	927.361419	222.8
TS CH → OH	927.5834964	175.4	927.385428	159.8
TS OH → NH	927.5980398	137.2	927.396419	131.0[b])
$CHNH^+$	928.02846738	0	927.8105340	0
TS $CHNH^+ \rightarrow CHOH^+$	927.96733530	38.36	927.7549230	34.89
$NHOH^+$	927.9759788	32.93	927.7600440	31.68

[a]) NH: NO_2 group points towards C–H; NH2: NO_2 group forms H-bond with pyridine N-atom; OH2: NO_2H points towards pyridine N-atom; OH is not shown, because NO_2H points away from both C–H and N–H and, therefore, probably is not involved in the reaction. [b]) After zero-point energy (ZPE) correction, this transition state is lower in energy than the OH2 minimum.

2.2. *Spectrophotometric Titration of* **1**. Protonation of **1** (CH) at the pyridine N-atom in aqueous acid gives its conjugate acid $CHNH^+$. To determine the acidity constant of $CHNH^+$, $K_{a,c}^{CHNH} = c_H c_{CH}/c_{CHNH}$, at 25° and ionic strength $I = 0.1$M, we determined the UV spectra of **1** at *ca.* 50 pH values between 2 and 6 by titration in AcONa buffer (*Fig. 2*). Factor analysis of the complete set of spectra indicated that two components were sufficient to reproduce the observed spectra (240–320 nm) within experimental accuracy. A titration function was then fitted to the reduced data (*Exper. Part*). Three independent measurements gave an average $pK_{a,c}^{CHNH}$ value of 4.18 ± 0.02. *Wettermark* had reported a value of 4.1 [11]. The thermodynamic acidity constant

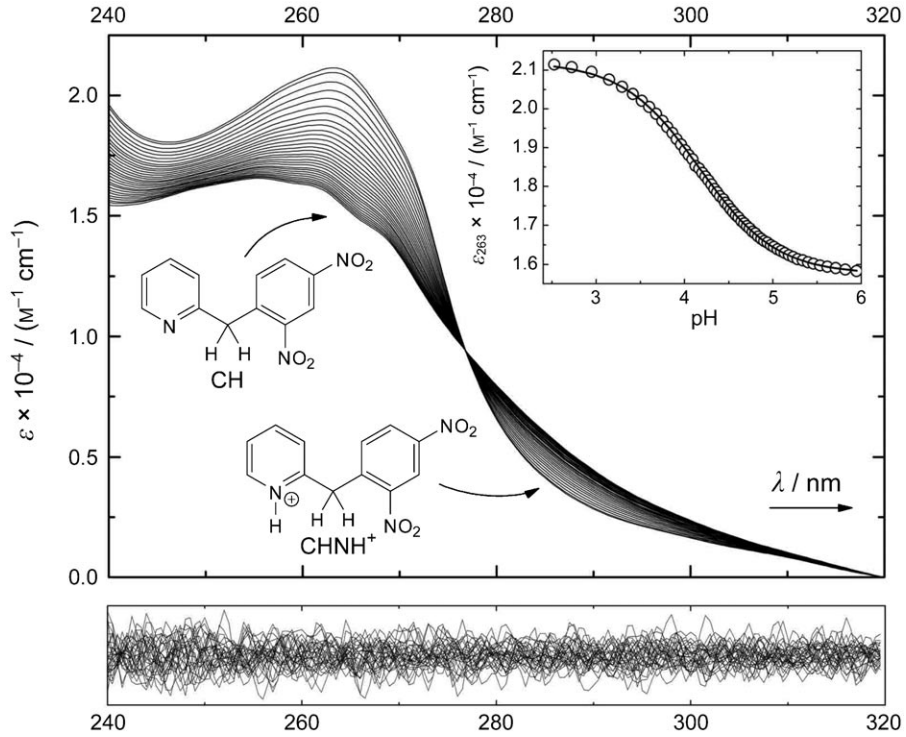

Fig. 2. *Spectrophotometric titration of* **1** *by stepwise addition of 0.1*M *NaOH to an aqueous solution containing 0.1*M *HCl, 0.1*M *AcONa, and* **1** (3×10^{-5} M) *at 25.0 ± 0.3°. Inset:* Absorbances at 263 nm (circles) and the globally fitted titration function (solid line). *Bottom Traces:* The residuals (scale: $\pm 1 \times 10^{-3}$ absorbance units) between the measured spectra and those reconstructed from two spectral components are white noise indicating that they arise from random errors of the spectrometer readings, rather than from a systematic error of the two-component titration model used for analysis.

K_a^{CHNH} should be close to the concentration quotient $K_{a,c}^{CHNH}$ determined here, because the dissociation $CHNH^+ \rightarrow CH + H^+$ is a charge-shift reaction.

2.3. *Flash Photolysis of* **1** *in Aqueous Solutions.* Acidic solutions ($pH \leqslant 3$) of **1** were excited with a pulsed ArF excimer laser (248 nm), and solutions with $pH > 3$ with a conventional discharge flashlamp. Transient absorption in the visible region was formed within 30 ns. The spectrum of the transient intermediate changed with pH: the maximum absorbance was at 520 nm for pH values below 6 and at 420 nm at higher pH, indicating a protonation equilibrium, $NH \rightleftharpoons CNO^- + H^+$. An estimate of the corresponding acidity constant, $pK_{a,c}^{NH} \approx 6.1 \pm 0.4$, was obtained by fitting a titration function to the initial transient absorbances at 420 and 520 nm that were observed at various pH (*Fig. 3*). Absorbance data obtained at $pH < 5$ were not considered for fitting, because protonation of **1** in the ground-state lowers the yield of the photoreaction. While the acidity constant of NH so obtained is less accurate than the value determined independently from kinetic data (*vide infra*), it does establish that ionization of NH occurs at $pH \approx 6$.

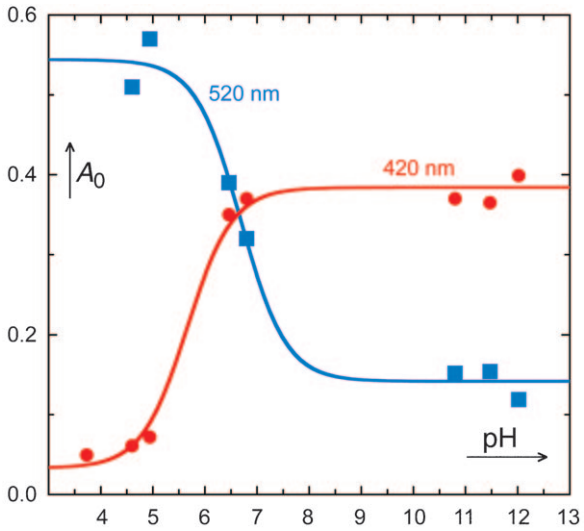

Fig. 3. *Initial transient absorbances observed by flash photolysis at 420 and at 520 nm in solutions of various pH*. Least-squares fitting of a titration function (solid lines) to the data points gave $pK_{a,c}^{NH} \approx 6.1 \pm 0.4$.

The decay of these transient intermediates obeyed the first-order rate law accurately, and the rate constants strongly depended on pH. In buffer solutions (pH 3.5–8.3), the rate increased with increasing buffer concentration, so that buffer dilution plots at constant buffer ratio were required to determine rate constants pertaining to wholly aqueous solution by extrapolation to zero buffer concentration. All solutions were adjusted to an ionic strength of $I = 0.1$M by addition of NaCl. The pH-dependent rate constants k_{obs}^{in} so obtained are given in *Table S1* of the *Supplementary Material*[2]) and are plotted in *Fig. 4*.

3. Discussion. – The acid–base and tautomeric equilibria of 2-(2,4-dinitrobenzyl)-pyridine (**1**) are summarized in *Scheme 2*; the experimental data underlying the acidity and equilibrium constants given in the *Scheme* will be discussed below. All equilibrium constants are concentration quotients, K_c, valid for ionic strength $I = 0.1$M. The *N*-protonated conjugate acid of CH, $CHNH^+$, is identical with the *C*-protonated conjugate acid of NH. The common conjugate base resulting from *C*-deprotonation of CH, *N*-deprotonation of NH, or *O*-deprotonation of OH is labeled CNO^-. The acidity constant of $CHNH^+$ was determined by spectrophotometric titration (*Fig. 2*), $pK_{a,c}^{CHNH} = 4.18 \pm 0.02$.

Irradiation of CH is expected to yield the *aci*-nitro tautomer OH (top of *Scheme 2*) as the primary photoproduct. Correspondingly, the conjugate acid of CH, $CHNH^+$, is expected to yield $NHOH^+$ (bottom left). The photoproduct OH is a strong oxygen acid. Its acidity constant can be estimated using the thermodynamic cycle CH → OH →

[2]) The *Supplementary Material* can be obtained upon request from the authors or from the Editorial Office.

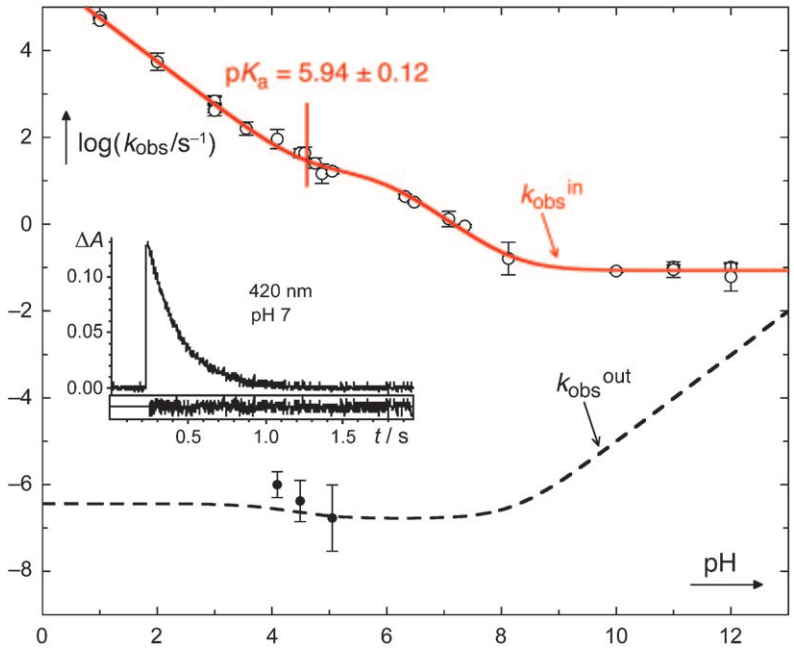

Fig. 4. *pH–Rate profile for the decay* (k_{obs}^{in}) *of the transient absorption generated by flash photolysis of* **1** *in aqueous solutions at ambient temperature* ($21 \pm 2°$). The solid line was determined by nonlinear least-squares fitting of *Eqn. 5* that will be derived in the *Discussion*. The *Inset* shows a kinetic trace determined in phosphate buffer, pH 7. The dotted line at the bottom represents the pH–rate profile for the reverse reaction (k_{obs}^{out}), which was calculated from *Eqn. 9* using the parameters given in *Table 2* (*vide infra*). The three data points shown near the bottom line (*) are the intercepts of the buffer dilution plots for the iodination rates of **1** reported in the thesis by *Quirke* [21].

$CNO^- + H^+ \rightarrow CH$, *i.e.*, $pK_{a,c}^{OH} = pK_{a,c}^{CH} - pK_T^{OH} \approx -0.6$. The equilibrium constant for the light-induced tautomerization $CH \rightarrow OH$, $pK_T^{OH} \approx 14.5$, was obtained from density-functional calculations for the lowest-energy OH form [8] ignoring entropy, *i.e.*, $pK_T \approx E_{rel}/(\ln(10)RT)$, $\ln(10)RT = 5.71$ kJ mol^{-1}. The ionization constant of CH, $pK_{a,c}^{CH} = 13.94$, will be derived below. The cation $NHOH^+$ must be an even stronger acid, being the conjugate acid of OH that carries an extra positive charge at the pyridine N-atom. Such strong oxygen acids will protonate H_2O on a time scale [24] not resolved by nanosecond flash photolysis ($\leqslant 30$ ns), whereby $NHOH^+$ yields the enamine NH, and OH yields the anion CNO^-. Intramolecular proton transfer from OH to NH is unlikely to compete in aqueous solution. In any case, on time scales exceeding 10^{-4} s, which are of interest here, we observed only the transient intermediate NH and its conjugate base CNO^-.

Proton transfer involving a C-atom is generally much slower than proton transfer between two heteroatoms (O and N) [24][25]. Hence, the ionization equilibrium $NH \rightleftharpoons CNO^- + H^+$ will be established prior to protonation of either of these species at the bridging C-atom. In other words, we assume that all the protonation equilibria

Scheme 2. *Ionization and Tautomerization Equilibria of* **1** *in Aqueous Solution*

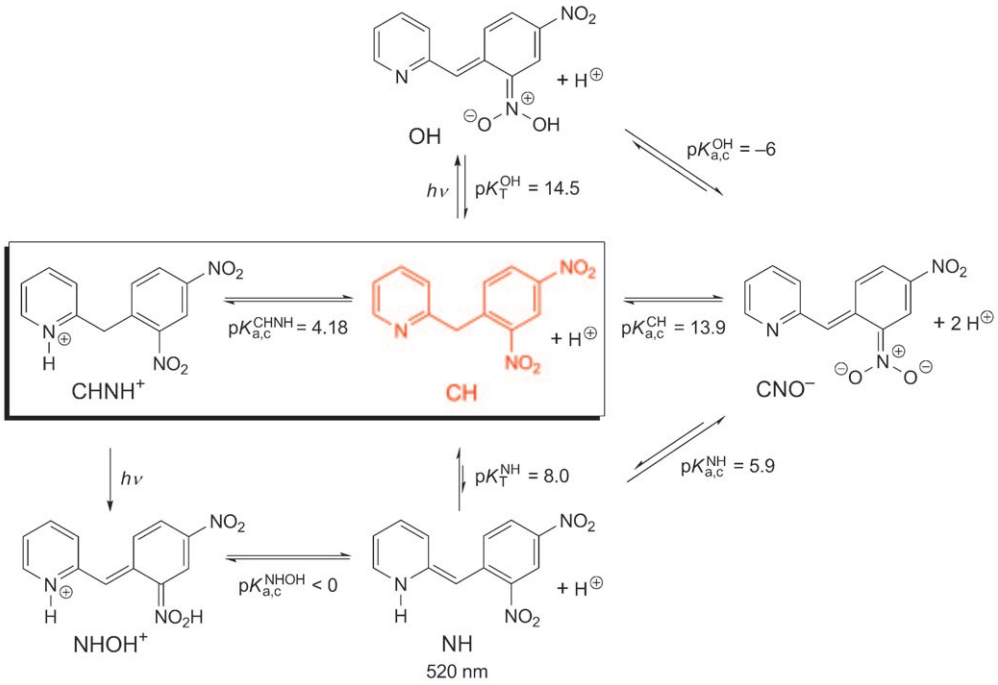

involving transient species (those placed outside of the box drawn around the stable species CH and $CHNH^+$ in *Scheme 2*) are established within the lifetimes of NH and its conjugate base CNO^-.

To derive the rate laws governing the tautomerization reactions of **1**, we focus on the rate-determining proton transfer reactions involving a C-atom, which are defined in *Scheme 3*. The upper index of the rate constants k designates the product formed by proton transfer, the lower index defines the acid (H_2O, H^+, or general acid HA in the presence of a buffer) or the base (H_2O, OH^-, or general base A^-) involved. For example, k_{HA}^{CH} is the second-order rate constant for the reaction of a general acid HA with CNO^- yielding CH and A^-. The constants k_0 for reactions with solvent H_2O are first-order rate constants.

Scheme 3. *Microscopic Rate Constants for the Rate-Determining Proton-Transfer Reactions Connecting* $CHNH^+$ *with NH, and CH with* CNO^-

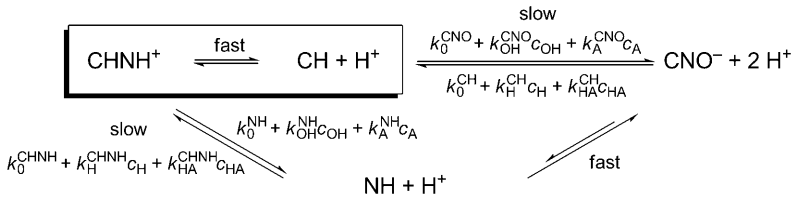

The six individual reactions that transfer species *into* the box are protonation of NH or of CNO^- by the three available acids H_2O, H^+, and HA. Adding up all these contributions we obtain the total rate v^{in} (*Eqn. 1*):

$$v^{in} = (k_0^{CHNH} + k_H^{CHNH} c_H + k_{HA}^{CHNH} c_{HA}) c_{NH} + (k_0^{CH} + k_H^{CH} c_H + k_{HA}^{CH} c_{HA}) c_{CNO} \quad (1)$$

We define the total concentration of the equilibrated transient intermediates formed by flash photolysis (drawn outside of the black box in *Scheme 3*) as $c_{tot}^{out} = c_{NH} + c_{CNO}$. Using the acidity quotient of NH, $K_{a,c}^{NH} = c_H c_{CNO}/c_{NH}$, we can express the two variables c_{NH} and c_{CNO} of *Eqn. 1* as pH-dependent fractions of c_{tot}^{out} (*Eqns. 2* and *3*).

$$c_{NH} = c_{tot}^{out}/(1 + K_{a,c}^{NH}/c_H) \quad (2)$$

$$c_{CNO} = c_{tot}^{out}/(1 + c_H/K_{a,c}^{NH}) \quad (3)$$

The rate v^{in} is seen to be a first-order rate law, $v^{in} = k^{in} c_{tot}^{out}$, where the first-order rate constant k^{in} (*Eqn. 4*) is a function of the concentration of protons, c_H, and of the general acid, c_{HA}. These variables remain essentially constant during the decay of a given transient, provided that the concentrations of acid, base, or buffer are much larger than those of the reacting species.

$$k^{in} = \frac{(k_0^{CHNH} + k_H^{CHNH} c_H + k_{HA}^{CHNH} c_{HA}) c_H + (k_0^{CH} + k_H^{CH} c_H + k_{HA}^{CH} c_{HA}) K_{a,c}^{NH}}{c_H + K_{a,c}^{NH}} \quad (4)$$

In the absence of a buffer, $c_{HA} = 0$M, *Eqn. 4* simplifies to *Eqn. 5*.

$$k^{in} = \frac{(k_0^{CHNH} + k_H^{CHNH} c_H) c_H + (k_0^{CH} + k_H^{CH} c_H) K_{a,c}^{NH}}{c_H + K_{a,c}^{NH}} \quad (5)$$

The rate of the reverse reaction v^{out} transferring the equilibrated species $CHNH^+$ and CH from inside the box of *Scheme 2* to the reactive intermediates NH and CNO^- *outside*, is derived in the same way. We define $c_{tot}^{in} = c_{CH} + c_{CHNH}$, and express c_{CH} and c_{CHNH} as fractions of c_{tot}^{in} (*Eqns. 6* and *7*),

$$c_{CH} = c_{tot}^{in}/(1 + c_H/K_{a,c}^{CHNH}) \quad (6)$$

$$c_{CHNH} = c_{tot}^{in}/(1 + K_{a,c}^{CHNH}/c_H) \quad (7)$$

to obtain the rate law $v^{out} = k^{out} c_{tot}^{in}$ with the first-order rate constant k^{out} (*Eqn. 8*) where the ionization constant of water is $K_w = c_H c_{OH} = 1.59 \times 10^{-14}$ M^2 at ionic strength $I =$ 0.1M.

$$k^{out} = \frac{(k_0^{NH} + k_{OH}^{NH} K_w/c_H + k_A^{NH} c_A) c_H + (k_0^{CNO} + k_{OH}^{CNO} K_w/c_H + k_A^{CNO} c_A) K_{a,c}^{CHNH}}{c_H + K_{a,c}^{CHNH}} \quad (8)$$

This reduces to *Eqn. 9* in the absence of a buffer, $c_A = 0$.

$$k^{out} = \frac{k_0^{NH} c_H + k_{OH}^{NH} K_w + (k_0^{CNO} + k_{OH}^{CNO} K_w / c_H) K_{a,c}^{CHNH}}{c_H + K_{a,c}^{CHNH}} \quad (9)$$

The observable decay rate of excess concentrations $c_{tot}^{out}(t)$ formed by flash photolysis at time $t = 0$ is equal to the difference between the rates of the forward and backward reaction (*Eqn. 10*). Equilibrium ($t = \infty$) is reached when $v^{in} = v^{out}$, *i.e.*, when $-dc_{tot}^{out}(t)/dt = 0$.

$$-dc_{tot}^{out}(t)/dt = v^{in} - v^{out} = k^{in} c_{tot}^{out}(t) - k^{out} c_{tot}^{in}(t) \quad (10)$$

Integration of *Eqn. 10* gives *Eqn. 11*.

$$-\ln\left[\frac{c_{tot}^{out}(t) - c_{tot}^{out}(\infty)}{c_{tot}^{out}(0) - c_{tot}^{out}(\infty)}\right] = (k^{in} + k^{out})t \quad (11)$$

In the present case, the decay of the transient species CN and CNO^- is practically irreversible, $k^{in} \gg k^{out}$, so that the rate constant $k_{obs}^{in} = k^{in} + k^{out}$ obtained by flash photolysis of **1** is close to k^{in}, except for strongly basic solutions, where pH approaches $pK_{a,c}^{CH}$ and CNO^- becomes the predominant species at equilibrium. The parameters of *Eqn. 5* were thus determined by nonlinear least-squares fitting of the function (k^{in}/s^{-1}) to the logarithm of the observed first-order rate constants (*Table S1*). The resulting values of the five independent parameters are given in *Table 2* (*Entries 1–4*). Two terms with the same pH-dependence are combined in *Entry 3* of *Table 2*; we consider this dichotomy below. The fitted function $\log(k^{in}/s^{-1})$ is plotted as a solid line in the pH–rate profile (*Fig. 4*). It reproduces the data accurately.

The pH-independent segment (slope 0) on the right-hand side of the pH–rate profile (pH > 8) represents the protonation of CNO^- by H_2O. Acid catalysis (slope −1) sets in at pH < 8 due to either or both of the processes $CNO^- + H^+ \rightarrow CH$, represented by the microscopic rate constant k_H^{CH}, and *C*-protonation of NH by H_2O, k_0^{CHNH}. Catalysis by these processes reaches a plateau as pH decreases below the $pK_{a,c}^{NH} = 5.94$, where the equilibrium between CNO^- and NH shifts towards the latter. However, acid catalysis (slope −1) takes over again at pH < 4, where the reaction $NH + H^+ \rightarrow CHNH^+$, represented by k_H^{CHNH} (*Entry 1*) predominates.

The reverse reaction described by *Eqn. 8* can be rendered irreversible and, thereby, observable, by trapping the short-lived products NH and CNO^-. *More O'Ferrall* and *Quirke* [21] have measured rate constants for the iodination of **1** in AcOH buffers, buffer ratios $R = c_{HA}/c_A = 3$, 1.19, and 1/3, as a function of acetate concentration c_A. The slopes and intercepts of the buffer dilution plots were determined from the original data given in the thesis of *Quirke* (*Table S3*[2])). We have determined buffer dilution plots for the rate constant k_{obs}^{in} for the same buffers by flash photolysis (*Tables S2*[2])). The nominal pc_H values of these buffers ($I = 0.1$M) are 4.09, 4.49, and 5.05, respectively.

Equilibrium ($t = \infty$) between the species inside and outside of the box (*Scheme 2*) is reached, when the rates of the forward and backward reactions are equal,

Table 2. *Best Values of the Equilibrium and Rate Constants Determined in This Work*

Entry	Parameter	Value	Source
1	k_H^{CHNH}	$(5.8 \pm 0.5) \times 10^5$ M^{-1} s^{-1}	pH–Rate profile, *Eqn. 5*
2	$K_{a,c}^{NH}$; $pK_{a,c}^{NH}$	$(1.2 \pm 0.4) \times 10^{-6}$ M; 5.94 ± 0.14	pH–Rate profile, *Eqn. 5*[a])
3	$k_H^{CH}\ K_{a,c}^{NH} + k_0^{CHNH}$	(17 ± 4) s^{-1}	pH–Rate profile, *Eqn. 5*
4	k_0^{CH}	(0.09 ± 0.01) s^{-1}	pH–Rate profile, *Eqn. 5*
5	$K_{a,c}^{CHNH}$; $pK_{a,c}^{CHNH}$	$(6.6 \pm 0.3) \times 10^{-5}$ M; 4.18 ± 0.02	Titration (*Fig. 2*)
6	pK_T^{OH}	~14.5	DFT Calculation [8]
7	K_T^{NH}; pK_T^{NH}	$(1.0 \pm 0.1) \times 10^{-8}$; 8.00 ± 0.05	*Table S3, Eqn. 12*[b])
8	$pK_{a,c}^{CH}$	13.94 ± 0.15	$pK_{a,c}^{NH} + pK_T^{NH}$
9	k_{HA}^{CHNH}	$(3.0 \pm 0.1) \times 10^4$ M^{-1} s^{-1}	*Table S2*, *Eqn. 13*
11	k_0^{NH}	$(3.8 \pm 0.2) \times 10^{-8}$ s^{-1}	$k_H^{CHNH}\ K_{a,c}^{CHNH}\ K_T^{NH}$
12	k_{OH}^{CNO}	$(6.8 \pm 0.4) \times 10^{-2}$ M^{-1} s^{-1}	$k_0^{CH}\ K_{a,c}^{NH}\ K_T^{NH}/K_w$
13	$k_{OH}^{NH}\ K_w + k_0^{CNO}\ K_{a,c}^{CHNH}$	$(1.1 \pm 0.3) \times 10^{-11}$ M s^{-1}	$(k_H^{CH}\ K_{a,c}^{NH} + k_0^{CHNH})\ K_{a,c}^{CHNH}\ K_T^{NH}$

[a]) Titration using the initial absorbances A_0 determined by flash photolysis (*Fig. 3*) gave $pK_{a,c}^{NH} = 6.1 \pm 0.4$. [b]) A value of 8.1 was given in [21].

$k^{out}c_{tot}^{in}(\infty) = k^{in}c_{obs}^{out}(\infty)$ (*Eqn. 10*). The ratios $c_{tot}^{out}(\infty)/c_{tot}^{in}(\infty) = k^{out}/k^{in}$ are, however, a function of pH, as is reflected in *Fig. 4*: The two pH–rate profiles are not parallel, the distance between the upper and lower curve, $\log(k^{out}) - \log(k^{in}) = \log(k^{out}/k^{in})$ is a function of pH. To determine the pH-independent equilibrium constant $K_T^{NH} = c_{NH}(\infty)/c_{CH}(\infty)$ from the observed rate constants, we replace $c_{NH}(\infty)$ and $c_{CH}(\infty)$ using *Eqns. 2* and *6* to obtain *Eqn. 12*, in which the ratio $k^{out}/k^{in} = c_{tot}^{out}(\infty)/c_{tot}^{in}(\infty)$ (*Eqn. 10*) is modified by factors accounting for the partial removal of CH and NH through protonation and deprotonation, respectively.

$$K_T^{NH} = \frac{1 + c_H/K_{a,c}^{CHNH}}{1 + K_{a,c}^{NH}/c_H} \frac{c_{tot}^{out}(\infty)}{c_{tot}^{in}(\infty)} = \frac{1 + c_H/K_{a,c}^{CHNH}}{1 + K_{a,c}^{NH}/c_H} \frac{k^{out}}{k^{in}} \tag{12}$$

The principle of microscopic reversibility (or its corollary, the principle of detailed balancing: in a system of connected reversible reactions at equilibrium, each reversible reaction is individually at equilibrium) assures that the same factor applies to all reaction pathways, in particular to the reactions catalyzed by general acids or bases in buffer solutions. The correction factors for the ratio k^{out}/k^{in} of the slopes of the buffer dilution plots (*Eqn. 12*) were calculated using the acidity constants $K_{a,c}^{NH}$ and $K_{a,c}^{CHNH}$ given in *Table 2* and the nominal pc_H values given in *Table S2*. They amount to 2.2, 1.4, and 1.0 for the three buffers, respectively. Applying *Eqn. 12* to the slopes of the three buffer dilution plots (*Table S3*) gave an average tautomerization constant $K_T^{NH} = (1.0 \pm 0.05) \times 10^{-8}$, $pK_T^{NH} = 8.00 \pm 0.05$.[3])

[3]) It should be mentioned that the ionic strength I was not held constant, but low ($I \leqslant 0.03$M), in the work of *More O'Ferrall* and *Quirke* [21]. The required activity coefficients will partly, but not completely, cancel in *Eqn. 12*. The systematic error arising from the neglect of this correction should amount to no more than -0.1 units of K_T^{NH}.

Eqn. 12 can also be used to determine the tautomerization constant K_T^{NH} from the intercepts of the buffer dilution plots for the rate constants of iodination, k^{out} (*Table S3*), and of transient decay, k^{in} (*Table S2*). The values obtained from the intercepts are less accurate, but fully consistent, $pK_T^{NH} = 7.9 \pm 0.2$.

Tautomerization of CH to NH, followed by ionization of the latter, amounts to ionization of CH as a carbon acid: $pK_T^{NH} + pK_{a,c}^{NH} = pK_{a,c}^{CH} = 13.94 \pm 0.20$, again in satisfactory agreement with an estimate of *More O'Ferrall* and *Quirke* ($pK_a^{CH} = 14.1$) [21]. Their direct measurement of pK_a^{CH} was hampered by irreversible reactions of **1** occurring in strongly basic solutions [26].

The slopes of the buffer dilution plots of transient decay correspond to the derivative of *Eqn. 4* with respect to the buffer-acid concentration c_{HA} (*Eqn. 13*).

$$\frac{\partial k^{in}}{\partial c_{HA}} = \frac{k_{HA}^{CHNH} c_H + k_{HA}^{CH} K_{a,c}^{NH}}{c_H + k_{a,c}^{NH}} \tag{13}$$

The slopes $\partial k^{in}/\partial c_{bu}$ for AcOH buffer are given in *Table S2* and $\partial k^{in}/\partial c_{HA} = \partial k^{in}/\partial c_{bu}(1 + 1/R)$, where R is the buffer ratio c_{HA}/c_{A^-}. A plot of $\partial k^{in}/\partial c_{HA}(c_H + K_{a,c}^{NH})$ *vs.* c_H accurately obeyed the expected linear relationship with a slope of $k_{HA}^{CHNH} = (3.0 \pm 0.1) \times 10^4$ M^{-1} s^{-1} and an ill-defined intercept of $k_{HA}^{CH} K_{a,c}^{NH} = (1.8 \pm 30) \times 10^{-3}$ s^{-1}. Thus, buffer-acid catalysis is dominated by the process $CNO^- + HA \rightarrow CH + A^-$ in the pH-range of the AcOH buffer.

We return to *Entry 3* of *Table 2*, $k_H^{CH} K_{a,c}^{NH} + k_0^{CHNH}$, which combines two independent mechanistic paths with the same dependence on c_H, namely $CNO^- + H^+ \rightarrow CH$ and $NH \rightarrow CHNH^+ + OH^-$. The contribution by the second reaction increases with acid concentration, because the pre-equilibrium concentration of NH increases linearly with c_H as long as $pH \gg pK_{a,c}^{NH}$. To obtain an *a priori* estimate for the relative contributions of the two terms, we use *Marcus*' expression [27] (*Eqn. 14*).

$$k = k_d \exp(-\Delta G^{\ddagger}/RT), \text{ where } \Delta G^{\ddagger} = \Delta G_0^{\ddagger}[1 + \Delta G^0/(4\Delta G_0^{\ddagger})]^2 \tag{14}$$

The parameter $\Delta G_0^{\ddagger}$ is the 'intrinsic' barrier, the barrier of a thermoneutral proton transfer reaction ($\Delta G^0 = 0$) to the C-atom. It was determined as $\Delta G_0^{\ddagger} = 57 \pm 2$ kJ mol^{-1} from an extensive set of ketonization rates of enols using $k_d = 1 \times 10^{11}$ M^{-1} s^{-1} for the diffusional rate constant of protons in H_2O [25]. The standard free-energy change of the first reaction, $CNO^- + H^+ \rightarrow CH$, amounts to $\Delta G^0 = -2.303RTpK_{a,c}^{CH} = -80$ kJ mol^{-1}. *Eqn. 14* gives $k_H^{CH} = 7 \times 10^6$ M^{-1} s^{-1}, and the product $k_H^{CH} K_{a,c}^{NH}$ amounts to 8 s^{-1}. To evaluate the second term, we need the equilibrium constant for the protonation of NH by solvent H_2O, $NH \rightarrow CHNH^+ + OH^-$, which amounts to $K_w/(K_{a,c}^{CHNH} K_T^{NH})$, $\Delta G^0 = 2.303RT(pK_w - pK_{a,c}^{CHNH} - pK_T^{NH}) = 9.3$ kJ mol^{-1}. *Eqn. 14* then predicts 1.8 M^{-1} s^{-1} for the second-order rate constant for protonation of NH by H_2O. Multiplication with the concentration of H_2O gives $k_0^{CHNH} = 100$ s^{-1}, which is an order magnitude higher than that for $k_H^{CH} K_{a,c}^{NH}$ obtained above. Thus, both estimates are close to the observed magnitude of the sum $k_H^{CH} K_{a,c}^{NH} + k_0^{CHNH} = 16.4$ s^{-1} (*Table 2*, *Entry 3*) and too close to each other to warrant a clear-cut identification of the dominant term.

Finally, we can now determine the parameters of *Eqn. 9*, the pH–rate profile for the thermal reaction rate k_{obs}^{out}. The rate constants k_0^{NH} and k_H^{CHNH} stand for the forward reaction $CHNH^+ \rightarrow NH + H^+$ and its reverse, repectively. Their ratio, k_0^{NH}/k_H^{CHNH}, is thus equal to the dissociation constant for the reaction $CHNH^+ \rightarrow NH + H^+$, which, in turn, is equal to $K_{a,c}^{CHNH}K_T^{NH}$. Hence, $k_0^{NH} = k_H^{CHNH}K_{a,c}^{CHNH}K_T^{NH} = (3.8 \pm 0.2) \times 10^{-7}\ s^{-1}$. Similarly, k_{OH}^{CNO} and k_0^{CH} are the rate constants for the reaction $CH + OH^- \rightarrow CNO^-$ and its reverse, respectively. Hence, $k_{OH}^{CNO} = k_0^{CH}K_T^{NH}K_{a,c}^{NH}/K_w = (6.8 \pm 0.4) \times 10^{-2}\ M^{-1}\ s^{-1}$. Finally, $(k_{OH}^{NH}K_w + k_0^{CNO}K_{a,c}^{CHNH}) = (k_0^{CHNH} + k_H^{CH}K_{a,c}^{NH})K_{a,c}^{CHNH}K_T^{NH} = (1.1 \pm 0.3) \times 10^{-11}\ M\ s^{-1}$.

The complete set of the rate and equilibrium constants relevant for the tautomerization reactions (*Scheme 3*) of 2-(2,4-dinitrobenzyl)pyridine (**1**) determined in this work is collected in *Table 2* and the resulting pH–rate profiles of the rate constants for the forward (k_{obs}^{in}) and backward (k_{obs}^{out}) reactions are shown in *Fig. 4*.

The properties of DNBP (**1**) are in principle suited for its application as a proton shuttle in an artificial membrane as depicted in *Fig. 1*. However, improvement of the reversibility of the photochromic reaction and of the lifetime of the NH form by structural variation such as replacement of the pyridine ring by a nitrogen heterocycle with a higher basicity are probably needed for a practical application.

Experimental Part

1. *Spectrophotometric Titration.* Absorption spectra were recorded with a *Perkin-Elmer Lambda 9* spectrophotometer. The temp. was maintained within $25 \pm 0.3°$, with a thermostated cell-holder. An optical quartz cell equipped with a magnetic stirrer was filled with 2 ml of an aq. soln. containing **1** (2×10^{-5} M), 0.1M AcONa, and 0.1N HCl. A microprocessor-controlled *Metrohm LL* micro pH glass electrode (*Biotrode*) was calibrated with standard *Metrohm* buffer solns. (pH 4, 7, 9 [28]) before each set of measurements. Portions (50 µl) of the titrant (0.1N NaOH) were added directly to the quartz cell inside the spectrophotometer using *Metrohm*'s *725 Dosimat* equipped with an *806*-exchange unit (10-cm^3 cylinder). A magnetic stirrer inside the cell ensured rapid mixing. Following each addition of titrant, a spectrum was recorded after the time required to maintain the drift of the pH electrode within 0.01 pH units per min. About 50 spectra and pH readings were collected during each titration. Titrations were conducted at constant ionic strength $I = 0.1$M. The resulting acidity constants are, therefore, dissociation quotients $K_{a,c}$ at $I = 0.1$M.

The spectra were corrected for dilution and analyzed with the help of the program SPECFIT [29], which performs factor analysis of the complete data matrix and allows to calculate acidity constants as optimized model parameters, together with their standard errors, by nonlinear least-squares fitting to a titration function.

2. *Conventional Flash Photolysis.* Transient kinetics were measured on an instrument of conventional design. The excitation flash of 50-µs width at half-height was produced by an electrical discharge of 1000-J energy through two parallel quartz tubes of 16-cm length and 1-cm diameter. A 20-V quartz-iodine lamp powered by a stabilized supply was used as a monitoring light source. The signals were detected by an *EMI 9685 B* photomultiplier, passed to the 50-Ω input of a *Tektronix* transient digitizer *TDS 540*, and processed by nonlinear least-squares fitting a first-order rate law.

We are most grateful to Prof. *R. More O'Ferrall* for providing a copy of the thesis by *A. P. Quirke* and for helpful discussions.

REFERENCES

[1] A. E. Tschitschibabin, B. M. Kuindshi, S. W. Benewolenskaja, *Ber. Dtsch. Chem. Ges.* **1925**, *58*, 1580.
[2] M. Schwörer, J. Wirz, *Helv. Chim. Acta* **2001**, *84*, 1441; Y. V. Il'ichev, M. A. Schwörer, J. Wirz, *J. Am. Chem. Soc.* **2004**, *126*, 4581.
[3] J. D. Margerum, L. J. Miller, E. Saito, M. S. Brown, H. S. Mosher, R. Hardwick, *J. Phys. Chem.* **1962**, *66*, 2434.
[4] E. Klemm, D. Klemm, *J. Prakt. Chem.* **1979**, *321*, 407.
[5] J. Kleinschmidt, A. Graness, *J. Photochem.* **1983**, *22*, 25.
[6] K. Kuldová, A. Corval, H. P. Trommsdorff, J. M. Lehn, *J. Phys. Chem. A* **1997**, *101*, 6850.
[7] a) K. Yokoyama, T. Kobayashi, *Chem. Phys. Lett.* **1982**, *85*, 175; b) H. Takahashi, S. Hirukawa, S. Suzuki, Y. Torii, H. Isaka, *J. Mol. Struct.* **1986**, *146*, 91.
[8] P. Naumov, K. Sakurai, T. Ishikawa, J, Takahashi, S.-y. Koshihara, Y. Ohashi, *J. Phys. Chem. A* **2005**, *109*, 7264.
[9] P. Naumov, A. Sekine, H. Uekusa, Y. Ohashi, *J. Am. Chem. Soc.* **2002**, *124*, 8540.
[10] H. S. Mosher, E. R. Hardwick, D. Ben Hur, *J. Chem. Phys.* **1962**, *37*, 904; D. Ben-Hur, R. Hardwick, *J. Chem. Phys.* **1972**, *57*, 2240.
[11] G. Wettermark, *J. Am. Chem. Soc.* **1962**, *84*, 3658.
[12] E. Klemm, D. Klemm, A. Graness, J. Kleinschmidt, *J. Prakt. Chem.* **1979**, *321*, 415; E. Klemm, D. Klemm, A. Graness, J. Kleinschmidt, *Chem. Phys. Lett.* **1978**, *55*, 113.
[13] A. Corval, R. Casalegno, O. Ziane, H. D. Burrows, *J. Phys. Chem. A* **2002**, *106*, 4272.
[14] J. Takeda, D. D. Chung, J. Zhou, K. A. Nelson, *Chem. Phys. Lett.* **1998**, *290*, 341.
[15] I. Frank, S. Grimme, S. D. Peyerimhoff, *J. Phys. Chem.* **1996**, *100*, 16187; S. Khatib, S. Tal, O. Godsi, U. Peskin, Y. Eichen, *Tetrahedron* **2000**, *56*, 6753.
[16] E. Klemm, D. Klemm, J. Reichardt, H.-H. Hörhold, *Z. Chem.* **1973**, *13*, 375; D. Klemm, E. Klemm, *J. Prakt. Chem.* **1979**, *321*, 404; D. Klemm, E. Klemm, K. Schüler, H.-H. Hörhold, *J. Prakt. Chem*. **1977**, *319*, 647.
[17] S. Houbrechts, K. Clays, A. Persoons, Z. Pikramenou, J.-M. Lehn, *Chem. Phys. Lett.* **1996**, *258*, 485.
[18] D. Gust, T. A. Moore, A. L. Moore, *Acc. Chem. Res.* **2001**, *34*, 40.
[19] K. Kinbara, T. Aida, *Science* **2006**, *313*, 51.
[20] P. J. Haberfield, *J. Am. Chem. Soc.* **1987**, *109*, 6178.
[21] R. More O'Ferrall, A. P. Quirke, *Tetrahedron Lett.* **1989**, *30*, 4885.
[22] G. N. Andreev, B. Schrader, D. A. Hristozova, V. B. Delchev, J. S. Petrov, P. Rademacher, *J. Mol. Struct.* **2003**, *645*, 77.
[23] I. Frank, D. Marx, M. Parrinello, *J. Phys. Chem. A.* **1999**, *103*, 7341.
[24] M. Eigen, *Angew. Chem.* **1963**, *75*, 489; *Angew. Chem., Int. Ed.* **1964**, *3*, 1.
[25] J. Wirz, *Pure Appl. Chem.* **1998**, *70*, 2221; J. Wirz, *Chem. Unserer Zeit* **1998**, *32*, 311.
[26] R. A. More O'Ferrall, personal communication.
[27] A. O. Cohen, R. A. Marcus, *J. Phys. Chem.* **1968**, *72*, 4229.
[28] H. Sigel, A. D. Zuberbühler, O. Yamauchi, *Anal. Chim. Acta* **1991**, *255*, 63.
[29] H. Gampp, M. Maeder, C. J. Meyer, A. D. Zuberbühler, *Talanta* **1985**, *32*, 95, 257, and 1133; H. Gampp, M. Maeder, C. J. Meyer, A. D. Zuberbühler, *Talanta* **1986**, *33*, 943.

Received May 20, 2009